Mol Biotechnol (2014) 56:1110–1120
DOI 10.1007/s12033-014-9791-8

RESEARCH

Virus-Like Particles from *Escherichia coli*-Derived Untagged Papaya Ringspot Virus Capsid Protein Purified by Immobilized Metal Affinity Chromatography Enhance the Antibody Response Against a Soluble Antigen

Jesús Guerrero-Rodríguez · Carlos Alberto Manuel-Cabrera · Y. Apatzingan Palomino-Hermosillo · Paola Guadalupe Delgado-Guzmán · Martha Escoto-Delgadillo · Laura Silva-Rosales · Sara Elisa Herrera-Rodríguez · Carla Sánchez-Hernández · Abel Gutiérrez-Ortega

Published online: 14 August 2014

Abstract There is a growing interest in using virus-like particles (VLPs) as scaffolds for the presentation of antigens of choice to the immune system. In this work, VLPs from papaya ringspot virus capsid protein expressed in *Escherichia coli* were evaluated as enhancers of antibody response against a soluble antigen. Interestingly, although the capsid protein lacks a histidine tag, its purification by immobilized metal affinity chromatography was achieved. The formation of VLPs was demonstrated by electron microscopy for the first time for this capsid protein. VLPs were enriched by polyethylene glycol precipitation. Additionally, these VLPs were chemically coupled to green fluorescent protein in order to evaluate them as antigen carriers; however, bioconjugate instability was observed. Nonetheless, the adjuvant effect of these VLPs on BALB/c mice was evaluated, using GFP as antigen, resulting in a significant increase in anti-GFP IgG response, particularly, IgG1 class, demonstrating that the VLPs enhance the immune response against the antigen chosen in this study.

Keywords Papaya ringspot virus · Capsid protein · Virus-like particles · Adjuvant · Antibody response

Introduction

Viruses have been extensively explored as tools for medicine, such as nucleic acid delivery, gene transfer technology, cancer therapy, medical materials and devices, imaging, and vaccine development [1]. Due to their

Electronic supplementary material The online version of this article (doi:10.1007/s12033-014-9791-8) contains supplementary material, which is available to authorized users.

J. Guerrero-Rodríguez · M. Escoto-Delgadillo · C. Sánchez-Hernández
Centro Universitario de Ciencias Biológicas y Agropecuarias, Universidad de Guadalajara, Carretera Guadalajara-Nogales km 15.5, 45110 Zapopan, Jalisco, Mexico
e-mail: guerreroajf@hotmail.com

M. Escoto-Delgadillo
e-mail: edm00897@cucba.udg.mx

C. Sánchez-Hernández
e-mail: shc32289@cucba.udg.mx

C. A. Manuel-Cabrera · P. G. Delgado-Guzmán · S. E. Herrera-Rodríguez · A. Gutiérrez-Ortega (✉)
Unidad de Biotecnología Médica y Farmacéutica, Centro de Investigación y Asistencia en Tecnología y Diseño del Estado de Jalisco A.C., Normalistas 800, Colinas de la Normal, 44270 Guadalajara, Jalisco, Mexico
e-mail: aortega@ciatej.mx

C. A. Manuel-Cabrera
e-mail: caalmaca_07@hotmail.com

P. G. Delgado-Guzmán
e-mail: pdelguz85@gmail.com

S. E. Herrera-Rodríguez
e-mail: sherrera@ciatej.mx

Y. A. Palomino-Hermosillo
Unidad de Tecnología de Alimentos, Secretaría de Investigación y Posgrado, Universidad Autónoma de Nayarit, Boulevard Tepic-Xalisco S/N, 63155 Tepic, Nayarit, Mexico
e-mail: pasingan@gmail.com

L. Silva-Rosales
Departamento de Ingeniería Genética, Centro de Investigación y de Estudios Avanzados del Instituto Politécnico Nacional Unidad Irapuato, Libramiento Norte km 9.6, Carretera Irapuato-León, 36821 Irapuato, Guanajuato, Mexico
e-mail: lsilva@ira.cinvestav.mx

nanometric scale, viral particles (VPs) and virus-like particles (VLPs) are considered as particulate matter in vaccine formulations; therefore, they are more readily internalized by antigen-presenting cells (APCs) and stimulate MHC-I and -II responses, priming long-lasting T- and B-cell immunity [2]. For this reason, a variety of animal, plant, and bacterial VPs and VLPs has been evaluated as scaffold and platform for antigen carrying, delivery, and release to the main cells of the immune system [3]. VLPs are formed by one or several viral proteins that self-assemble, mimicking the morphology of VPs, but devoid of genomic material, making VLPs non-infective and non-pathogenic. Viral capsid proteins (CPs), which assemble into VLPs, have been widely used to present foreign epitopes on their surface for vaccine development. The properties of VLPs, like size, shape, surface charge, repetitiveness in a geometric pattern, encapsulation of small molecules, along with the availability of diverse techniques to manipulate VLPs surface, such as translational fusions and chemical conjugation, make these particles suitable for increasing the immune response against proteins and peptides that are poor immunogens [4]. The chemical conjugation approach is used for the attachment of larger peptides or complete proteins to the surface of VLPs, in comparison with the translational fusion approach that generally allows the insertion of no more than 20 amino acids without compromising self-assembly of the capsid protein [5]. Due to the accessibility of lysine and cysteine residues on VLPs, chemical conjugation has been achieved using different linkers [6]. Chemical conjugation represents the most effective strategy currently available for selective and orientation-controlled functionalization of nanoparticles; however, controlling the reaction in terms of ligand density remains a challenge [7].

Plant virus CPs are attractive candidates as polypeptide presentation systems, since plant viruses are often easy to grow in large quantities, purification is usually straightforward, and many CPs are stable. Also, genetically modified plant virus CPs have been expressed in various heterologous systems [8]. A series of contributions describing epitope presentation in the surface of plant viruses have been reviewed by Plummer and Manchester [9]. Currently, the mainly studied plant viruses for this purpose are Cowpea Mosaic Virus (CPMV) (reviewed in [10, 11]), Tobacco Mosaic Virus (TMV) [12], and Papaya Mosaic Virus (PapMV) [13]. The first two viruses, along with Turnip Yellow Mosaic Virus (TYMV), Maize Rayado Fino Virus (MRFV), and Tobacco Etch Virus (TEV), have also been studied as scaffolds for protein presentation through chemical modification [14–18].

Potyviruses are flexuous filamentous plant viruses, ranging from 700 to 900 nm long and 11–15 nm wide. The virion is formed with approximately 2,000 copies of the CP, which ranges from 28 to 40 kDa mass weight, depending mainly on the virus N-terminal length [19]. The Potyvirus CPs possess interesting features that offer potential to their use as vaccine carriers: the N- and C-termini are exposed on the surface of the virion, the N-terminus varies in length and sequence depending on the virus, the core region is conserved with a few variations, virus particles can be dissociated in monomers and reassembled to form virions (i.e., with encapsulated RNA) or VLPs (i.e., without RNA), and N- and C-termini can be removed from virus particles without affecting their structure [20, 21]. Hence, modifications in N- and/or C-termini of the CP might contribute to the display of attached molecules on the surface, without affecting particle formation or disrupting the core particle. To this respect, some potyviruses, such as Plum Pox Virus (PPV), Johnson Grass Mosaic Virus (JGMV), and Potato Virus Y (PVY), have been evaluated as antigen and peptide presentation platforms [22–24].

Papaya ringspot virus (PRSV) is a member of the potyvirus group and its CP N-terminus presents 11 repeats of negatively–positively charged amino acids, predominantly, glutamic acid and lysine [25]. PRSV CP has been previously investigated as peptide carrier. Chatchen and co-workers analyzed the presentation of an antigenic peptide from canine parvovirus into the CP of PRSV. A sequence encoding a 15-amino acid epitope of VP2 protein was inserted at the 5′ and/or 3′ ends of PRSV *cp* gene, and the chimeric proteins were expressed in *Escherichia coli* [26]. It was found that PRSV CP was able to increase the antibody response against the presented epitope when it was injected into mice. This work also exposes the presence of lysines in the surface of the PTVs, which can be used for chemical conjugation of antigens. In the present work, we achieved the expression of PRSV CP in *E. coli* and its purification as VLPs, the chemical coupling of VLPs to green fluorescent protein (GFP), and assessed the adjuvant effect of such VLPs, through the measurement of GFP-specific antibody titer.

Materials and Methods

Cloning of PRSV Capsid Protein in Bacterial Expression Vector

Nucleotide sequence of native *cp* gene from a PRSV isolate, denominated PRSVCP-Jal15, was previously cloned into plasmid pCR2.1-TOPO (Life Technologies). A pair of primers (IDT) was designed, by adding a NcoI cleavage site, a translation start and a glycine codon in the sense primer (5′ AAAAAACCATGGGAAATGAAGCTGTGGA TGCCGGT 3′), and a XhoI cleavage site was introduced to

the antisense primer (5′ GAACTCGAGTCAGTTGCG CATACCCAGGAG 3′). The PCR reaction was performed as follows: 1 cycle at 98 °C for 30 s, 30 cycles at 98 °C for 10 s, 52 °C for 30 s, and 72 °C for 1 min, and 1 cycle at 72 °C for 5 min, using 200 μM dNTPs, 0.5 μM forward and reverse primers, 1 μl of template plasmid, and 0.5 μl of Phusion HF DNA Polymerase (New England Biolabs) in a 25 μl reaction. The amplified product was purified with MinElute PCR Purification Kit (Qiagen), digested with NcoI/XhoI enzymes (New England Biolabs), purified with MinElute Gel Extraction Kit (Qiagen), and ligated to pET28a (+) prokaryotic expression vector (Novagen) using T4 DNA ligase (New England Biolabs). Plasmid construction, named pET28-PRSVcp, was confirmed by PCR using the primers mentioned above, by restriction pattern with NcoI/XhoI enzymes and also by DNA sequencing.

Expression of PRSV Capsid Protein in *E. Coli* and Verification by ELISA and WB

Chemically competent *E. coli* One Shot BL21Star (DE3) cells (Life Technologies) were transformed with pET28-PRSVcp plasmid. In order to optimize capsid protein expression, a set of experiments, using three different temperatures (23, 30, and 37 °C) and two different IPTG (Promega) concentrations (0.5 and 1 mM), was carried out as follows: a fresh colony was taken from a LB medium agar plate and placed in 3 ml of liquid LB/kanamycin medium (50 μg/ml) and incubated overnight at 37 °C and 250 rpm. Then, 200 μl of overnight culture was transferred to 5 ml of fresh LB liquid medium and incubated at 250 rpm for 4 h at the different temperatures and IPTG concentrations. Non-induced culture was used as control. Samples were collected every hour to monitor protein expression. Thereafter, cells were collected by centrifugation (4 °C, 15 min and 4,470×*g*), resuspended in 1:10 of the original culture volume with phosphate buffered saline (PBS) (Sigma-Aldrich) supplemented with 0.1 % Triton X-100 and Complete EDTA-free protease inhibitor cocktail (Roche) and lysed by 10 rounds of 10 s pulses with XL-2000 Sonicator (Misonix) at half potency. Total protein lysate was analyzed by SDS-PAGE and Coomassie Blue staining.

Additionally, total protein lysate was centrifuged (4 °C, 20 min and 4,470×*g*), and soluble/insoluble fractions were analyzed for PRSV CP expression by ELISA, using PRSV DAS ELISA kit (Agdia). Also, Western blot was performed using anti-PRSV alkaline phosphatase enzyme conjugate (Agdia) as detection antibody and BCIP/NBT alkaline phosphatase (Sigma-Aldrich) as substrate for color development. Western blot experiment was conducted in Tris buffer (100 mM Tris, 150 mM NaCl, pH 7.4).

Purification of PRSV CP Virus-Like Particles

After incubation at 30 °C and 1 mM IPTG *E. coli*-pET28-PRSVcp, PRSV CP was purified by immobilized metal affinity chromatography (IMAC) with a 1 ml His Trap HP column (GE Healthcare) by following manufacturer's instructions. Briefly, 250 ml culture grown in 1 l Erlenmeyer flask was used. Cell disruption was carried out as above in 25 ml of binding buffer (10 mM Tris, 300 mM NaCl, 20 mM imidazole, pH 7.2) supplemented with protease inhibitor. Lysate was centrifuged (4 °C, 20 min and 4,470×*g*) and passed through a Millex-HN 0.45 μm filtering unit (Merck-Millipore). Binding was done by applying the cleared lysate to pre-equilibrated column, followed by a washing step with 30 column volumes (CV) of washing buffer (10 mM Tris, 300 mM NaCl, 40 mM imidazole, and pH 7.2). For the elution step, 6 CV of elution buffer (10 mM Tris, 300 mM NaCl, 500 mM imidazole, and pH 7.2) were added. An additional elution step was performed with buffer containing 10 mM Tris, 300 mM NaCl, 1 M imidazole, and pH 7.2. Samples were collected at each step for monitoring the process of purification. Washing buffer flow-through was collected in 5 CV fractions, and the elution volume was collected in 0.5CV fractions. All fractions were analyzed by SDS-PAGE, and the presence of PRSV CP was confirmed by ELISA.

For enrichment of PRSV CP VLPs, fractions 2 and 3 from the first elution step were dialyzed against phosphate buffer (10 mM sodium phosphate, 300 mM NaCl, 10 mM EDTA, and pH 7.2) in 14 kDa MWCO nitrocellulose tubing (Sigma-Aldrich) for 12 h at 4 °C. Dialyzed sample was precipitated with 4 % (w/v) PEG 8000 for 1 h at 4 °C with constant shaking and left for 1 h at room temperature. Afterwards, the sample was centrifuged (4 °C, 30 min, 7,800×*g*) and the precipitate was solubilized in phosphate buffer. Finally, the VLPs were concentrated with a 30 kDa MWCO Amicon Ultra-4 filtration centrifugal unit (Merck-Millipore) by following manufacturer's instructions. Samples were collected at each step for monitoring the precipitation and concentration processes by SDS-PAGE. Protein concentration was estimated with Bradford reagent (Sigma-Aldrich).

Electron Microscopy

Affinity-purified PRSV CP was diluted 1:1 (v/v) with 6 % phosphotungstic acid pH 6.8 and 3 μl of the mixture were loaded in a Formvar Film 300 square mesh copper grid (Electron Microscopy Science). TEM was conducted on EM208S/Morgagni (Philips/FEI) at a final magnification of 56,000×. Native PRSV virion preparation was used as control.

Preparation of Purified GFP

Recombinant GFP was expressed in *E. coli* BL21Star strain (Life Technologies) transformed with plasmid pIVEX-GFP (Roche), as previously reported [27]. GFP expression was induced at 30 °C for 6 h with IPTG and its purification was carried out by affinity chromatography using Bio-Scale™ Mini Profinity™ IMAC 5 ml Cartridges (Bio-Rad). GFP was finally dialyzed against phosphate buffer (10 mM phosphate, 300 mM NaCl, 10 mM EDTA, and pH 7.2).

Conjugation of PRSV VLPs to GFP

A series of experiments were performed to assess adduct formation. First, GFP and PRSV CP VLPs were tested for sulfhydryl and amine group availability, respectively, for chemical conjugation. 100 M excess of maleimide-PEG_2-biotin and sulfo-NHS-SS-biotin (Thermo-Scientific) was reacted with GFP and PRSV CP VLPs, respectively, according to the provider's protocol. Reactions took place at room temperature for 2 h for GFP and several time points, from 10 to 60 min, for PRSV CP VLPs. Reaction products were analyzed by SDS-PAGE and Western blot assay with HRP-streptavidin (Sigma-Aldrich) for detection. For conjugation, GFP and PRSV CP VLPs were blocked with a 25 M excess of sulfo-NHS-acetate and a 5 M excess of *N*-ethylmaleimide (Thermo-Scientific), respectively, for 1 h at room temperature. Thereafter, blocked proteins were desalted with 10 kDa MWCO (for GFP) and 30 kDa MWCO (for PRSV CP VLPs) Amicon Ultra-4 filtration units (Merck-Millipore). Then, blocked GFP and PRSV CP VLPs were mixed together in a 1:2 molar ratio in the presence of 4 different molar excesses (20, 40, 80, and 160) of heterobifunctional crosslinker sulfo-MBS (Thermo-Scientific) in a one-step reaction overnight at 4 °C. Conjugation products were analyzed by SDS-PAGE and Western blot using anti-6x HisTag monoclonal antibody (Roche) as detection antibody.

Immunization of Mice

Twenty-two 5-week-old female BALB/c mice (Harlan Laboratories) were divided into 5 groups of 4 mice and 1 control group of 2 mice. Groups were immunized with 10 μg of GFP (GFP), 1 μg of PRSV (VLP), 10 μg of GFP mixed with complete Freund's adjuvant (Sigma-Aldrich) for priming and incomplete Freund's adjuvant (Sigma-Aldrich) for boosting (GFP-FA), a mixture of 10 μg of GFP and 10 μg of PRSV (GFP-VLP10), a mixture of 10 μg of GFP and 1 μg of PRSV (GFP-VLP1) or phosphate buffer saline (PBS). All immunizations were carried out subcutaneously with 100 μl of the different preparations on day 1 and 15. Blood was collected by tail vein bleeding before immunization (bleeding 1), 14 and 30 days after first immunization (bleedings 2 and 3, respectively). Serum samples were obtained after two consecutive incubations of 1 h at 37 °C and 2 h at 4 °C and centrifugation (10 min, at room temperature, for $10{,}000\times g$) and were preserved at −80 °C until used. Mice care and maintenance were carried out in the Vaccine Evaluation Module of Animal Experimentation Facilities (Centro de Investigación y Asistencia en Tecnología y Diseño del Estado de Jalisco, Mexico) according to international protocols.

Titration of Anti-GFP Antibodies

Immune serum samples obtained after the immunization protocol were used to determine total IgG antibody response against GFP by ELISA. For the assay, serum samples for each group were pooled and diluted 1:100, 1:1,000, and 1:10,000 with blocking buffer (PBS, 0.05 % Tween-20, 5 % non-fat dry milk). First, 96-well MaxiSorp Immuno Plates (Nunc) were coated with 1 μg of GFP recombinant protein per well diluted in carbonate coating buffer (10 mM carbonates, pH 9.6), overnight at 4 °C. Thereafter, plates were blocked with blocking buffer for 2 h at room temperature and then washed once with washing buffer (PBS, 0.1 % Tween-20). 100 μl of diluted serum samples was added to the wells, and plates were incubated overnight at 4 °C. After six washes, 100 μl of HRP-donkey anti-mouse IgG (R&D Systems) diluted 1:1,000 in PBS, 0.05 % Tween-20, and 2.5 % non-fat dry milk was added and incubated 4 h at room temperature. After six washes, 150 μl of 3–3′, 5–5′ tetramethylbenzidine solution (Sigma-Aldrich) was added to each well, and color development was stopped after 10 min, using 150 μl of 1 N sulfuric acid solution. Finally, plates were read at 450 nm in xMark microplate absorbance spectrophotometer (Bio-Rad). The experiment was performed in duplicate. For anti-GFP antibody isotyping, serum sample pools were analyzed for their relative levels of mouse IgG1, IgG2a, and IgG2b isotypes, using a mouse monoclonal antibody isotyping kit (Sigma-Aldrich), by following the manufacturer's instructions for antigen-mediated ELISA. Briefly, coating was done with 1 μg of GFP per well. 100 μl of HRP-conjugated anti-goat IgG secondary antibody (Sigma-Aldrich) diluted 1:3,000 in PBS was added per well. Differences between groups were analyzed by one-way ANOVA followed by Tukey–Kramer test using JMP 8.0.2 program (SAS Institute Inc.).

Results and Discussion

Expression of PRSV CP in *E. coli*

Expression of PRSV CP in *E. coli* was confirmed by SDS-PAGE, ELISA, and Western blot. The PRSV CP monomer

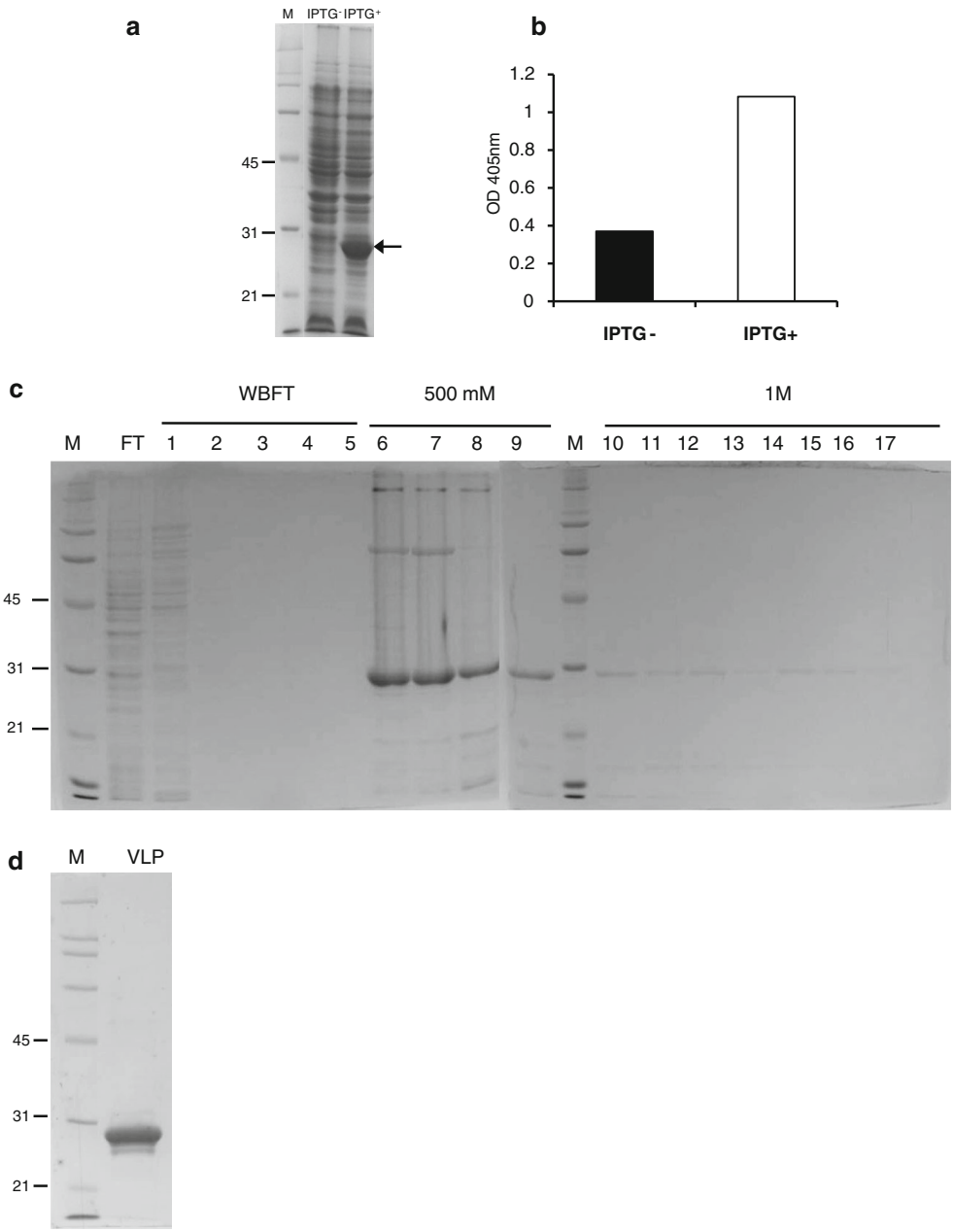

Fig. 1 Expression of PRSV CP in *E. coli* and purification. Total protein lysates from both induced (IPTG+) and uninduced (IPTG−) bacterial cultures were analyzed for the presence of PRSV CP by SDS-PAGE (**a**) and ELISA (**b**). **c** Purification of PRSV CP by IMAC. Fractions corresponding to each step of the process were analyzed by SDS-PAGE. FT: flowthrough, WBFT: washing buffer flowthrough, 500 mM: eluted fractions using 500 mM of imidazole, 1 M: eluted fractions using 1 M of imidazole. **d** PRSV CP VLPs enrichment. Purified PRSV CP was precipitated with PEG 8000, diafiltrated and analyzed by SDS-PAGE. *M* molecular weight markers in kDa

has theoretical molecular weight around 33 kDa, as calculated with CLC Main Workbench 6.0 (CLC Bio), which correlates with the abundant band present in the total protein lysate separated by SDS-PAGE in the induced *E. coli* culture (Fig. 1a). At the same time, PRSV CP expression in total lysate was confirmed by ELISA, using a commercially available kit (Fig. 1b). In order to determine whether the accumulation of PRSV CP was in soluble or insoluble fractions, both fractions were analyzed by SDS-PAGE and Western blot (Supplemental Fig. 1). PRSV CP accumulates predominantly in the insoluble fraction 4 h after induction with 1 mM IPTG at 37 °C. Since protein extraction from insoluble fraction usually denatures proteins, it was likely that no PRSV VLPs would form after PRSV CP refolding. Therefore, a series of experiments were performed with the aim of obtaining PRSV CP in the soluble fraction of induced cultures, testing different temperatures, and IPTG concentrations. The best conditions for PRSV CP expression in soluble fraction were 30 °C and 1 mM IPTG after 4 h of induction (Supplemental Fig. 2).

Purification of PRSV CP VLPs

IMAC was used for purification of PRSV CP from an *E. coli* culture that was induced with 1 mM IPTG at 30 °C. It was deduced that the presence of a patch of glutamic

acid-lysine repeat near the N-terminus of monomeric PRSV CP could be used for binding of PRSV CP to nickel ions immobilized in the IMAC column. The purification process was performed in Tris buffer with moderate ionic strength at near neutral pH. Binding of PRSV CP to the column was successful in the presence of imidazole (20 mM), with minimal losses of unbound PRSV CP. After several washing steps, most of *E. coli*-derived proteins were washed out from the column. Elution of PRSV CP was tested at different imidazole concentrations, starting at 150 mM imidazole (data not shown), where no PRSV CP was detected. Best results were obtained at 500 mM imidazole, where most of PRSV CP eluted at 0.5–2.5 column volume fractions. Noteworthily, minor contaminant proteins were observed. Also, high imidazole concentration (1 M) was tested for post-elution of PRSV CP after the 500 mM imidazole elution to assess total elution of protein of interest; however, low levels of PRSV CP were detected after this step (Fig. 1c). Thus, 500 mM imidazole is sufficient to elute most of the protein of interest. IMAC purification of native proteins (i.e., proteins with no affinity tag) has been carried out by others based on three principles: the protonated state of histidine amino acid in solution near physiologic pH, the protonated state of some negatively charged amino acid, like glutamic and aspartic acid, near neutrality, and the electrostatic interactions between the protein and the metal-ion-matrix complex [28]. In all three cases, the process depends on NaCl concentration, the presence of a competitor (e.g., imidazole), the pH of solution, and the protein pI in solution [29]. The high retention of PRSV CP in the column may be a consequence of one of the mentioned mechanisms. The monomeric form of PRSV CP possesses six histidines along the sequence and a balanced content of negatively (glutamic and aspartic acid) and positively (arginine and lysine) charged residues, with a frequency of 0.146 and 0.149, respectively, giving a pI in solution of 8.77. The N-terminus of PRSV capsid protein contains the 11 glutamic acid-lysine repeat, and this region is reported to be exposed on the surface of many potyviral particles [20], leading to the idea that glutamic acid could be interacting with metal-ion matrix; however, the retention of glutamic acid at physiological pH has not been observed. On the other hand, lysine and arginine have higher retention properties [29]. The attachment of lysine to the nickel matrix is a pH-dependent event, and lysine, arginine, and histidine selectively bind at pH 8.5–9.1 [30]. Theoretically, half of the glutamic acid-lysine dipeptide repeat is solvent exposed in the VLP, and it is possible that a specific environment at the VLP surface is created, in which the glutamic acid-lysine moiety can donate electrons at pH $\sim$7, thus binding to metal matrix due to the balance of protonated (positively charged)/deprotonated (negatively charged) state between the two amino acids. Glutamic acid-lysine dipeptide has been used as a buffer system with a pI 6.0 value in solution containing 2 % salt [31]; so, at pH values over 6.0, the peptide must be deprotonated. Another explanation comes from observations of cytidylyltransferase interacting with anionic, non-zwitterionic membranes, where glutamic acid contained in a long amphipathic α-helix with a net negative charge is weakly acidic, but lowering the pH induces its deprotonation, enabling it to interact with an anionic membrane [32]. Similarly, lysine of PRSV CP, in a context of a net positive charge, becomes deprotonated when the pH increases above the protein pI. Additionally, PRSV CP assembly into VLPs before column loading may contribute to a stronger binding, as a consequence of exposing more sites in the particle's surface for interaction with the metal matrix, requiring higher concentrations of imidazole to elute the particle. After IMAC purification, eluted PRSV CP was immediately dialyzed and VLP enrichment was performed with 4 % PEG 8,000 precipitation and diafiltration (30 kDa MWCO), since PRSV CP monomers could interfere with the conjugation analysis and the adjuvanticity effect experiments. In the same way, other filamentous viruses and some potyviruses have been successfully purified using PEG precipitation under the conditions used in the present work [33]. After all these steps, a highly pure VLP preparation can be observed by SDS-PAGE (Fig. 1d). This preparation has a concentration of 1.26 mg/ml, and the estimated overall yield is around 5 mg/l of culture medium, which is consistent with the yield reported for PVY VLP produced in *E. coli* [24].

Electron Microscopy of *E. coli*-Derived PRSV CP VLPs

After PRSV CP purification by IMAC, samples of purified protein were analyzed in a transmission electron microscope, to assess VLP formation. PRSV CP VLPs were observed under the microscope (Fig. 2a). The PRSV CP VLPs had an average of 200 nm in length and 10 nm in width, significantly shorter than native virus particles (780 nm $\times$ 12 nm) [34, 35]. However, compared with a native PRSV particle (Fig. 2b), the differences in size encountered in the formed VLPs are probably normal, since some native VPs have a length of 250 nm. Besides, like native VPs, the formed PRSV CP VLPs possess the typical form of flexuous filaments. The presence of few VLPs per field may be due to the high imidazole concentration (500 mM) from the purification process in the analyzed sample, which was not desalted before microscope observation. It is likely that this imidazole concentration destabilizes VLPs, leading to the formation of insoluble complexes, which were observed after storing the VLP sample at 4 °C in elution buffer.

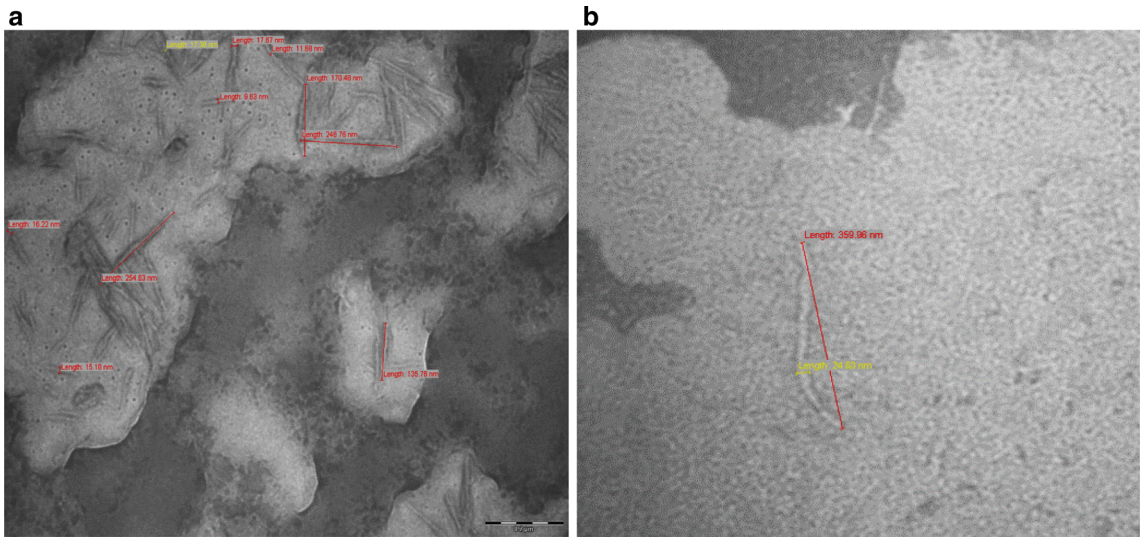

Fig. 2 Observation of PRSV CP VLPs by transmission electron microscopy. **a** *E. coli*-derived PRSV CP VLPs purified by IMAC. **b** Native PRSV particle

Chemical Coupling of PRSV CP VLPs to GFP

The idea of coupling GFP molecules to the PRSV CP VLPs was to test the capability of these VLPs as an addressable entity for chemical attachment of entire proteins on their surface without compromising the structure and stability of the generated bioconjugate. GFP was chosen as model protein in this study due to its ease of production, its highly stable fluorophore formation, and ease to evaluate its potential conformational changes through fluorescence emission [36].

The conjugation strategy involved the use of lysines in PRSV CP VLP and cysteines in GFP, and the availability of these groups was confirmed using NHS ester and maleimide compounds coupled to biotin, respectively (Fig. 3a, b). After confirming the presence of free groups for chemical crosslinking in both molecules, coupling of GFP to PRSV CP VLPs was conducted in phosphate buffer at pH 7.2, using heterobifunctional crosslinker MBS in a one-step reaction and confirmed by SDS-PAGE (Fig. 3c). Different crosslinker concentrations and reaction times were tested. The generation of PRSV CP VLP-GFP bioconjugate was successfully achieved using different concentrations of sulfo-MBS linker, as observed in SDS-PAGE analysis, comparing bioconjugation products of both proteins with non-blocked, non-conjugated GFP and non-blocked, non-conjugated PRSV CP PRSV. A protein of around 60 kDa in the middle part of the gel is the product of the coupling of GFP to PRSV CP VLPs, while the faint bands around it may be products with a different degree of linker incorporation. Also, unreacted GFP and PRSV CP monomers were observed. With these observations, the generation of bioconjugates between PRSV CP VLPs and GFP was confirmed. Once the PRSV CP VLP-GFP bioconjugate was generated, the formation of insoluble complexes after storage at 4 °C for a few hours was observed, indicating that the bioconjugate was not stable. A possible explanation for this is that the addition of many GFP molecules in the surface of PRSV CP VLPs destabilizes and disrupts the particle, resulting in the aggregation of insoluble bioconjugate complexes. Western blot assay was performed, using anti-His tag antibody to detect recombinant GFP, supporting this possibility (Fig. 3d). When 20- and 40-fold molar excesses of linker were added for conjugation, monomeric GFP disappeared completely, indicating its total coupling to the surface of PRSV CP VLPs. Conversely, when 80- and 160-fold molar excesses were added, the presence of GFP monomer and PRSV CP VLP-GFP conjugate were slightly visible only after the formation of insoluble complexes. Generation of stable bioconjugates has been successfully achieved in plant viruses, like the icosahedral CPMV [14, 37] and the rigid filamentous TMV [15, 38, 39]; however coupling efficiency and load capacity are not easy to estimate. When VPs are evaluated as carriers, loading capacity without compromising stability depends on the virus structure and size of the cargo. For the development of biological carriers, chemical coupling is actually the best controlled way of site-specific attachment, but loading capacity remains an important issue [21]. In this way, from a point of view of available sites for chemical coupling, filamentous viruses have a greater advantage due to the assembly of 2,000 copies of capsid protein, a number significantly shorter in spherical viruses. Nonetheless, flexous filamentous viruses appear to be less stable in structure than spherical ones [40]. Because of the instability of PRSV CP VLP-GFP bioconjugate, it was decided not to use this bioconjugate to immunize mice.

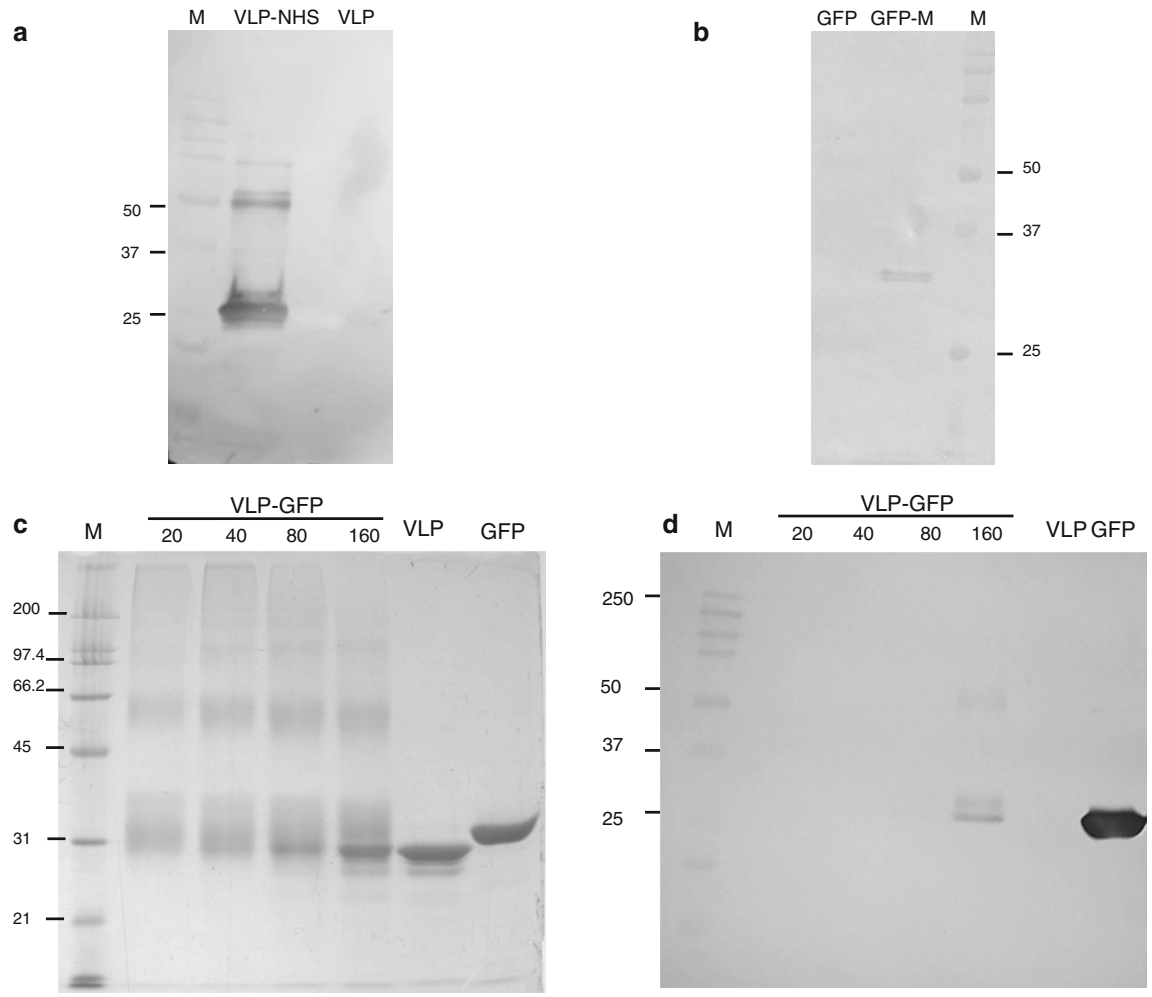

Fig. 3 Chemical coupling of VLPs to GFP. Amine and sulfhydryl group availability in VLPs (**a**) and GFP (**b**) with biotinylated compounds by Western blot. *VLP-NHS* VLPs reacted with sulfo-NHS-SS-biotin, *GFP-M* GFP reacted with maleimide-PEG2-biotin. Conjugation of VLPs to GFP, using 20, 40, 80, and 160 M excesses of sulfo-MBS crosslinker, was analyzed by SDS-PAGE (**c**) and Western blot (**d**). For comparison, either VLPs or GFP alone was reacted with the crosslinker. *M* molecular weight markers in kDa

GFP-Specific Antibody Production in Sera from Mice Immunized with PRSV CP VLPs Mixed with GFP

Immunization experiment was conducted to evaluate the adjuvant properties of PRSV CP VLPs in BALB/c mice using GFP as immunogen. Immunization, as well as bleeding scheme, is depicted in Fig. 4a. Two different PRSV:GFP ratios (1:1 and 1:10) were tested in order to evaluate dose-dependent adjuvanticity of PRSV CP VLPs. Initially, the antibody response was analyzed in either individual or pooled serum samples from immunized animals belonging to all the groups of study, and the results were similar (data not shown). For the above reason, anti-GFP IgG titers in pooled serum samples are reported. It was demonstrated that GFP-PRSV1 and GFP-PRSV10 mixtures induced a higher antibody response against GFP in comparison with GFP alone (Fig. 4b). No anti-GFP cross reaction was observed when PRSV alone was administered. A high antibody response against GFP was induced when Freund's adjuvant was used, even before boosting. In contrast, GFP-PRSV treatments induced a lower response than Freund's adjuvant treatment that was evident after boosting. Additionally, PRSV CP VLPs enhance antibody response against GFP in a dose-dependent manner, since a greater response is measured when GFP is administered along with 10 μg of VLPs. The GFP-specific IgG titer induced by this treatment was 1:1,000. Finally, anti-GFP IgG antibody isotyping revealed that IgG1 was the only isotype that was induced by the VLPs, like Freund's adjuvant, revealing a similar adjuvant mechanism than the latter (Fig. 4c).

GFP has been previously used as a model antigen in immunization experiments for evaluation of adjuvant effect

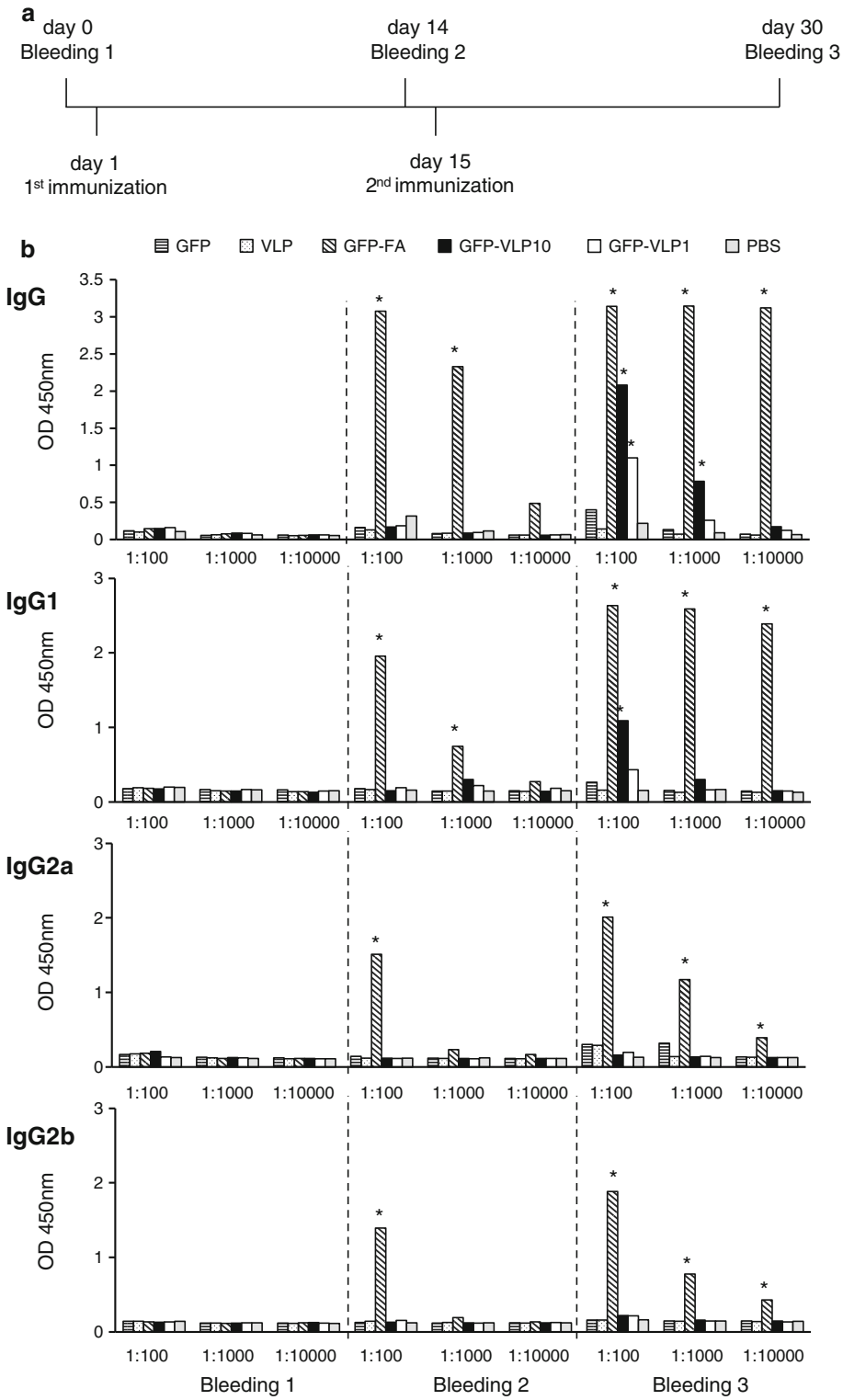

Fig. 4 Antibody response in mice immunized with a mixture of VLPs and GFP. **a** Immunization and bleeding scheme of the different groups. **b** Absorbance readings of anti-GFP IgG, IgG1, IgG2a, and IgG2b antibodies in serum samples of the different treatments. Samples were diluted 1:100, 1:1,000, and 1:10,000. *Asterisks* indicate the treatments that were statistically different from GFP treatment

of VPs or VLPs, either by genetic fusion or by chemical coupling to VLPs [15, 41]. The results obtained here with PRSV CP VLPs evaluated as an adjuvant are consistent with several works where antigenic peptides are fused to capsid protein of some plant viruses [12, 13, 42–46], and also plant potyviruses [22–24], where humoral/cellular-mediated antigen-specific IgG is enhanced after a second immunization. Here, the increase in antibody response against GFP, when administered along with PRSV CP VLPs to mice, may be a consequence of recruitment of

cells of innate immunity, which produces both cytokines and chemokines at the site of injection, a mechanism of action described in particulate adjuvants. Moreover, particulate adjuvants can also cause cell death and tissue injury in the site of administration, producing a strong inflammatory response [47]. PapMV VLPs co-administered with immunogenic peptides are efficiently processed by cells of the immune system, producing a balanced th1/th2 cytokine response. This observation leads to the idea of considering filamentous particles of PapMV as "pamptigens", defined as molecules recognized as pathogen-associated molecular patterns (PAMPs) by pattern recognition receptors (PRRs) [48, 49]. In the study of Savard and coworkers, a mixture of immunogenic peptide of seasonal influenza virus (SIV) with PapMV CP VLPs produced high peptide-specific antibody titer. Also, the administration of 30 μg of PapMV CP VLPs induced a higher humoral response compared with the administration of 3 μg of VLPs, resulting in 3.5- and 8-fold increase in IgG and IgG2a class response, respectively, which is an indicative of cell-mediated humoral response against SIV peptides due to the presence of PapMV VLPs [49].

Conclusion

PRSV CP VLPs have been successfully expressed in *E. coli*. Despite the fact that PRSV CP lacks a histidine tag, purification of the protein was achieved by IMAC, using nickel ions. Also, VLPs enrichment was performed by PEG precipitation and diafiltration. The formation of VLPs was demonstrated by electron microscopy. Additionally, PRSV VLPs were chemically coupled to a model antigen, GFP, however, bioconjugate instability was observed. Finally, the adjuvant effect of PRSV VLPs on BALB/c mice was evaluated, using GFP as antigen, resulting in a significant increase in anti-GFP IgG response, particularly, IgG1 class, suggesting that PRSV VLPs are able to recruit cells of the immune response to the site of injection, enhancing the response against the antigen chosen in this study.

Acknowledgments This research was supported by SEP-CONACYT Project 83863. Jesús Guerrero Rodríguez is indebted to CONACYT for the scholarship granted.

References

1. Yildiz, I., Shukla, S., & Steinmetz, N. F. (2011). Applications of viral nanoparticles in medicine. *Current Opinion in Biotechnology, 22*(6), 901–908.
2. Smith, D. M., Simon, J. K., & Baker, J. R. (2013). Applications of nanotechnology for immunology. *Nature Reviews Immunology, 13*(8), 592–605.
3. Ma, Y., Nolte, R. J., & Cornelissen, J. J. (2012). Virus-based nanocarriers for drug delivery. *Advanced Drug Delivery Reviews, 64*(9), 811–825.
4. Jennings, G. T., & Bachmann, M. F. (2008). The coming of age of virus-like particle vaccines. *Journal of Biological Chemistry, 389*(5), 521–536.
5. Jegerlehner, A., Tissot, A., Lechner, F., Sebbel, P., Erdmann, I., Kündig, T., et al. (2002). A molecular assembly system that renders antigens of choice highly repetitive for induction of protective B cell responses. *Vaccine, 20*(25–26), 3104–3112.
6. Smith, M. T., Hawes, A. K., & Bundy, B. C. (2013). Reengineering viruses and virus-like particles through chemical functionalization strategies. *Current Opinion in Biotechnology, 24*(4), 620–626.
7. Avvakumova, S., Colombo, M., Tortora, P., & Prosperi, D. (2014). Biotechnological approaches toward nanoparticle biofunctionalization. *Trends in Biotechnology, 32*(1), 11–20.
8. Johnson, J., Lin, T., & Lomonossoff, G. (1997). Presentation of heterologous peptides on plant viruses: Genetics, structure, and function. *Annual review of Phytopathology, 35*, 67–86.
9. Plummer, E. M., & Manchester, M. (2011). Viral nanoparticles and virus-like particles: Platforms for contemporary vaccine design. *Wiley Interdisciplinary Reviews: Nanomedicine and Nanobiotechnology, 3*(2), 174–196.
10. Brennan, F. R., Jones, T. D., & Hamilton, W. D. (2001). Cowpea mosaic virus as a vaccine carrier of heterologous antigens. *Molecular Biotechnology, 17*(1), 15–26.
11. Sainsbury, F., Cañizares, M. C., & Lomonossoff, G. P. (2010). Cowpea mosaic virus: The plant virus-based biotechnology workhorse. *Annual review of Phytopathology, 48*, 437–455.
12. Fitchen, J., Beachy, R. N., & Hein, M. B. (1995). Plant virus expressing hybrid coat protein with added murine epitope elicits autoantibody response. *Vaccine, 13*(12), 1051–1057.
13. Denis, J., Majeau, N., Acosta-Ramirez, E., Savard, C., Bedard, M. C., Simard, S., et al. (2007). Immunogenicity of papaya mosaic virus-like particles fused to a hepatitis C virus epitope: Evidence for the critical function of multimerization. *Virology, 363*(1), 59–68.
14. Chatterji, A., Ochoa, W., Shamieh, L., Salakian, S. P., Wong, S. M., Clinton, G., et al. (2004). Chemical conjugation of heterologous proteins on the surface of cowpea mosaic virus. *Bioconjugate Chemistry, 15*(4), 807–813.
15. Smith, M. L., Lindbo, J. A., Dillard-Telm, S., Brosio, P. M., Lasnik, A. B., McCormick, A. A., et al. (2006). Modified tobacco mosaic virus particles as scaffolds for display of protein antigens for vaccine applications. *Virology, 348*(2), 475–488.
16. Barnhill, H. N., Reuther, R., Ferguson, P. L., Dreher, T., & Wang, Q. (2007). Turnip yellow mosaic virus as a chemoaddressable bionanoparticle. *Bioconjugate Chemistry, 18*(3), 852–859.
17. Natilla, A., & Hammond, R. W. (2011). Maize rayado fino virus virus-like particles expressed in tobacco plants: A new platform for cysteine selective bioconjugation peptide display. *Journal of Virological Methods, 178*(1–2), 209–215.
18. Manuel-Cabrera, C. A., Márquez-Aguirre, A., Rodolfo, H. G., Ortiz-Lazareno, P. C., Chavez-Calvillo, G., Carrillo-Tripp, M., et al. (2012). Immune response to a potyvirus with exposed amino groups available for chemical conjugation. *Virology Journal, 9*, 75.
19. Dougherty, W. G., & Carrington, J. C. (1988). Expression and function of potyviral gene products. *Annual Review of Phytopathology, 26*, 123–143.
20. Shukla, D. D., Strike, P. M., Tracy, S. L., Gough, K. H., & Ward, C. W. (1988). The N and C termini of the coat proteins of potyviruses are surface-located and the N terminus contains the major virus-specific epitopes. *Journal of General Virology, 69*(7), 1497–1508.

21. Jagadish, M. N., Edwards, S. J., Hayden, M. B., Grusovin, J., Vandenberg, K., Schoofs, P., et al. (1996). Chimeric potyvirus-like particles as vaccine carriers. *Intervirology, 39*(1–2), 85–92.
22. Fernández-Fernández, M. R., Martínez-Torrecuadrada, J. L., Casal, J. I., & García, J. A. (1998). Development of an antigen presentation system based on plum pox potyvirus. *FEBS Letters, 427*(2), 229–235.
23. Saini, M., & Vrati, S. (2003). A Japanese encephalitis virus peptide present on Johnson grass mosaic virus-like particles induces virus-neutralizing antibodies and protects mice against lethal challenge. *Journal of Virology, 77*(6), 3487–3494.
24. Kalnciema, I., Skrastina, D., Ose, V., Pumpens, P., & Zeltins, A. (2012). Potato virus Y-like particles as a new carrier for the presentation of foreign protein stretches. *Molecular Biotechnology, 52*(2), 129–139.
25. Silva-Rosales, L., Becerra-Leor, N., Ruiz-Castro, S., Téliz-Ortiz, D., & Noa-Carrazana, J. C. (2000). Coat protein sequence comparisons of three Medican isolates of papaya ringspot virus with other geographical isolates reveal a close relationship to American and Australian isolates. *Archives of Virology, 145*(4), 835–843.
26. Chatchen, S., Juricek, M., Rueda, P., & Kertbundit, S. (2006). Papaya ringspot virus coat protein gene for antigen presentation in *Escherichia coli*. *Journal of Biochemistry and Molecular Biology, 39*(1), 16–21.
27. Rogé, J., & Betton, J. M. (2005). Use of pIVEX plasmids for protein overproduction in *Escherichia coli*. *Microbial Cell Factories, 4*, 18.
28. Charlton, A., & Zachariou, M. (2008). Immobilized metal ion affinity chromatography of native proteins, from: Methods in molecular biology. In M. Zachariou (Ed.), *Affinity chromatography: Methods and protocols* (Vol. 421). Totowa, NJ: Humana Press.
29. Sayeda-Hemdan, E., & Porath, J. (1985). Development of immobilized metal affinity chromatography: II. Interaction of amino acids with immobilized nickel iminodiacetate. *Journal of Chromatography A, 323*(2), 255–264.
30. Hemmasi, B. (1975). Ligand-exchange chromatography of amino acids on nickel-chelex 100. *Journal of Chromatography A, 104*(2), 367–372.
31. Cormier, M., Padmanabhan, R., Phipps, J. B., & Rauser, D. (2005). *Peptidically buffered formulations for electrotransport applications and methods of making, WO 2005051485 A1*. Mountain View, CA: Alza Corp.
32. Johnson, J. E., Xie, M., Singh, L. M. R., Edge, R., & Cornell, R. B. (2003). Both acidic and basic amino acids in an amphitropic enzyme, CTP: Phosphocholine cytidylyltransferase, dictate its selectivity for anionic membranes. *Journal of Biological Chemistry, 278*(1), 514–522.
33. Vajda, B. (1978). Concentration and purification of viruses and bacteriophages with polyethylene glycol. *Folia Microbiologica, 23*(1), 88–96.
34. Gonsalves, D., & Ishii, M. (1980). Purification and serology of papaya ringspot virus. *Phytopathology, 70*(11), 1028–1032.
35. Yeh, S. D., Jan, F. J., Chiang, C. H., Doong, T. J., Chen, M. C., Chung, P. H., et al. (1992). Complete nucleotide sequence and genetic organization of papaya ringspot virus RNA. *Journal of General Virology, 73*(Pt10), 2531–2541.
36. Chalfie, M. (1995). Green fluorescent protein. *Photochemistry and Photobiology, 62*(4), 651–656.
37. Gupta, S. S., Kuzelka, J., Singh, P., Lewis, W. G., Manchester, M., & Finn, M. G. (2005). Accelerated bioorthogonal conjugation: A practical method for the ligation of diverse functional molecules to a polyvalent virus scaffold. *Bioconjugate Chemistry, 16*(6), 1572–1579.
38. Schlick, T. L., Ding, Z., Kovacs, E. W., & Francis, M. B. (2005). Dual-surface modification of the tobacco mosaic virus. *Journal of the American Chemical Society, 127*(11), 3718–3723.
39. McCormick, A. A., Corbo, T. A., Wykoff-Clary, S., Palmer, K. E., & Pogue, G. P. (2006). Chemical conjugate TMV-peptide bivalent fusion vaccines improve cellular immunity and tumor protection. *Bioconjugate Chemistry, 17*(5), 1330–1338.
40. Grasso, S., & Santi, L. (2010). Viral nanoparticles as macromolecular devices for new therapeutic and pharmaceutical approaches. *International Journal of Physiology, Pathophysiology and Pharmacology, 2*(2), 161–178.
41. Fric, J., Marek, M., Hruskova, V., Holan, V., & Forstova, J. (2008). Cellular and humoral immune responses to chimeric EGFP-pseudocapsids derived from the mouse polyomavirus after their intranasal administration. *Vaccine, 26*, 3242–3251.
42. Joelson, T., Akerblom, L., Oxelfelt, P., Strandberg, B., Tomenius, K., & Morris, T. J. (1997). Presentation of a foreign peptide on the surface of tomato bushy stunt virus. *Journal of General Virology, 78*(Pt6), 1213–1217.
43. Modelska, A., Dietzschold, B., Sleysh, N., Fu, Z. F., Steplewski, K., Hooper, D. C., et al. (1998). Immunization Against Rabies with Plant-derived Antigen. *Proceedings of the National Academy of Sciences of the United States of America, 95*(5), 2481–2485.
44. Smolenska, L., Roberts, I. M., Learmonth, D., Porter, A. J., Harris, W. J., Wilson, T. M. A., et al. (1998). Production of a functional single chain antibody attached to the surface of a plant virus. *FEBS Letters, 441*(3), 379–382.
45. Brennan, F. R., Gilleland, L. B., Staczek, J., Bendig, M. M., Hamilton, W. D. O., & Gilleland, H. E, Jr. (1999). A chimeric plant virus vaccine protects mice against a bacterial infection. *Microbiology, 145*(Pt8), 2061–2067.
46. Natilla, A., Piazzolla, G., Nuzzaci, M., Saldarelli, P., Tortorella, C., Antonaci, S., et al. (2004). Cucumber mosaic virus as carrier of a hepatitis C virus-derived epitope. *Archives of Virology, 149*(1), 137–154.
47. Awate, S., Babiuk, L. A., & Mutwiri, G. (2013). Mechanisms of action of adjuvants. *Frontiers in Immunology, 4*, 114.
48. Acosta-Ramírez, E., Pérez-Flores, R., Majeau, N., Pastelin-Palacios, R., Gil-Cruz, C., Ramírez-Saldaña, M., et al. (2007). Translating innate response into long-lasting antibody response by the intrinsic antigen-adjuvant properties of papaya mosaic virus. *Immunology, 124*(2), 186–197.
49. Savard, C., Guérin, A., Drouin, K., Bolduc, M., Laliberté-Gagné, M. E., Dumas, M. C., et al. (2011). Improvement of the trivalent inactivated Flu vaccine using PapMV nanoparticles. *PLoS One, 6*(6), e21522.